

Type Ia Supernovae Standardization Beyond Light-Curve Corrections: An In-Depth Investigation into the Mass-step Implementation

Taeho Kim

Bergen County Academies, 200 Hackensack Ave, Hackensack, NJ 07601, United States

ABSTRACT

Type Ia supernovae (SNe Ia) serve as standardizable candles crucial for probing cosmic expansion and constraining cosmological parameters. SNe Ia have been standardized using their light-curves for nearly three decades, but more recent studies in the past 15 years have found that SN Ia brightnesses *after light-curve corrections* depend on their host-galaxy stellar masses. It has since become the standard to correct for this unexplained phenomenon by applying a ‘mass-step’ correction, where SNe Ia in host galaxies above a certain stellar-mass (mass-step location) are taken to be about 0.05 to 0.10 magnitudes (mag) or about 5 to 10% brighter than SNe Ia in host galaxies below the mass-step location. In this paper, three representative SN Ia surveys, the Dark Energy Survey 5 Year Supernova Analysis (DES-SN5YR), Pantheon+, and the Joint Light-curve Analysis (JLA) are analyzed and compared against each other. This work specifically focuses on the mass-step implementation in each of the surveys and how this correction impacts inferred cosmological parameters across varying redshifts.

Keywords: Type Ia Supernovae; Host-galaxy; Light curve; Mass-step; Dark Energy; Selection Effects

INTRODUCTION

Type Ia supernovae (SNe Ia) are thought to occur when a white dwarf in a binary system accretes mass from its companion until it reaches the Chandrasekhar limit (1). At the Chandrasekhar limit, or roughly 1.44 (solar masses), the white dwarf becomes unstable and explodes. It is because this critical mass is constant that the peak intrinsic SNe Ia luminosities are remarkably consistent, with an intrinsic dispersion estimated to be less than 0.2 mag (20% in terms of flux). SNe Ia have become essential tools for cosmology, serving as “standardizable

candles.” By comparing an SN Ia’s observed brightness with its expected luminosity, cosmologists can accurately determine distances to faraway galaxies. When these distances were matched with redshift measurements, or the amount the wavelength of light is stretched due to the expansion of the universe, in the late 1990s (2, 3), a striking discovery emerged: distant SNe Ia appeared dimmer than anticipated, implying that the universe’s expansion is accelerating.

This discovery challenged earlier assumptions about cosmic evolution: since the majority of the universe was assumed to consist of matter (both dark matter and ordinary, baryonic matter), it seemed natural that gravitational attraction would slow the universe’s expansion and potentially even cause it to contract. The relic responsible for the accelerating expansion of the universe was coined ‘dark energy.’ The nature of dark energy is unknown and is a topic of active research.

Corresponding author: TAEHO KIM, E-mail: taeho.nyop@hotmail.com.

Copyright: © 2026 TAEHO KIM. This is an open access article distributed under the terms of the Creative Commons Attribution License, which permits unrestricted use, distribution, and reproduction in any medium, provided the original author and source are credited.

Accepted May 26, 2026

<https://doi.org/10.70251/HYJR2348.43245254>

The measurement of some of the first SNe Ia above redshift 0.8 revealed unexpectedly low values for both the deceleration of cosmic expansion and the mass density thought to be responsible for the slowing of the expansion of the universe (4). More than a century ago, Einstein initially introduced the cosmological constant to describe a static universe, a notion he later abandoned upon learning that the universe is expanding. Modern observations have since reintroduced this constant, now associated with dark energy, which acts as a repulsive force that counteracts gravity. To disentangle the effects of mass and the cosmological constant, cosmologists analyzed a broad redshift range of SNe Ia. By plotting combinations of the matter and dark energy density parameters, consistent with each SN Ia's brightness, they could visualize how higher-redshift data help separate the effects of matter and dark energy (2, 3). The observations were consistent with a universe that decelerated during its first several billion years before transitioning to accelerated expansion, providing compelling evidence for the existence of dark energy. Establishing this result requires statistical rigor. A significance of at least 3σ is needed for the accelerating expansion to be considered highly probable, as this is 3 standard deviations away from the mean in a Gaussian (normal) distribution, with 99.7% of the data within this range. The first studies confirming the accelerating expansion of the universe were just above the 3σ threshold. Recent results from DES-SN5YR, or the Dark Energy Survey 5 Year Supernova Analysis however, reached a 5σ significance, meaning the probability of the result arising from random fluctuations is just two in a million (5). To further refine these cosmological parameters, cosmologists combine SNe Ia observations with other probes, such as gravitational lensing, the Cosmic Microwave Background (CMB), and Baryon Acoustic Oscillations (BAO).

To utilize SN Ia data for cosmology, the observed brightness must be standardized to reduce intrinsic variation and scatter. This standardization relies on analyzing the light-curve of each SN Ia to extract parameters describing its peak luminosity. An example of an SN Ia light-curve, or its brightness as a function of time, is shown in Figure 1. For example, in DES-SN5YR, SNe Ia were discovered using difference imaging and then calibrated via the forward global calibration method (6). The forward global calibration method is a cosmological fitting method in which all SN Ia light-curves and nuisance parameters are simultaneously optimized within a single forward model of the observed data, rather than calibrating each step separately.

Difference imaging is the process of subtracting a reference image of the sky, without the transient, from a new image to identify variable/new sources, such as SNe Ia. The standardized brightnesses can be related to cosmological parameters such as the matter content of the universe, as well as dark energy. A more detailed theoretical framework is presented in the Methods and Materials section.

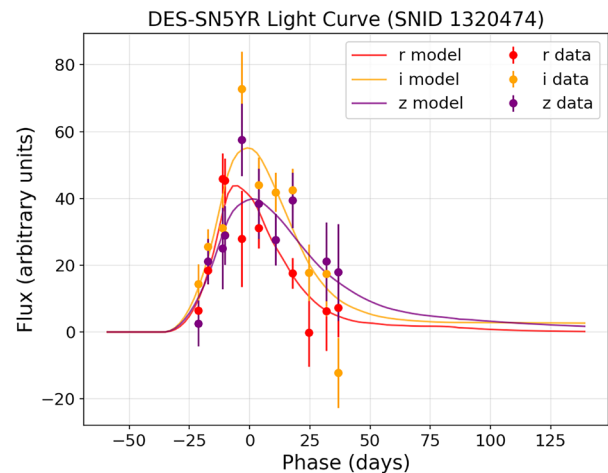


Figure 1. An example multi-band light-curve (brightness as a function of time) from DES-SN5YR. The circles denote the observations, while the lines are the best-fit light-curves from the SALT3 light-curve fitter. The stretch and color parameters from light-curve fitting are used to standardize SNe Ia. *riz* bands denote increasingly higher-wavelength bands, with the effective wavelengths being: 641 nm for the *r* band, 783 nm for the *i* band, and 926 nm for the *z* band.

A critical aspect of standardization is correcting for host-galaxy properties, such as stellar mass and color, which can subtly affect SN Ia brightnesses even after light-curve corrections are applied. A typical way this is accounted for is using the “mass-step”; SNe Ia in more massive galaxies tend to be brighter after light-curve corrections, a trend observed in multiple studies. Various surveys account for this in different ways: for example, the Supernova Legacy Survey (SNLS) found a mass-step size of ~ 0.08 mag, implemented with post-fit binning and cosmology fits (7), while JLA (8) performed the light-curve color and stretch corrections then fit for the host mass-step afterwards, and found a ~ 0.06 mag step. Pantheon+ and DES-SN5YR fit for the mass-step with bias corrections (which accounts for selection effects) simultaneously, and report mass step values of mag (9) and mag (5), respectively.

Some major interpretations on the underlying cause of the mass-step include progenitor effects, dust extinction effects, and bias corrections that model selection effects. Higher-mass galaxies tend to have older stellar populations and higher metallicities, which could impact the properties of SN Ia progenitors, affecting SN Ia luminosities even after light-curve standardization. Another interpretation is dust extinction effects, as Pantheon+ notes: different galaxies may have different dust distributions, which affect SN Ia color corrections and the observations used to plot the light-curve. Thus, standard light-curve models may not fully correct for dust effects. This is because dust absorbs light and re-emits it at longer wavelengths with lower energy, often making the light appear redder than the intrinsic color of the object. A third interpretation, present in both Pantheon+ and DES-SN5YR, is bias corrections. Because DES-SN5YR and Pantheon+ include detailed bias corrections modeled simultaneously with the mass-step, it becomes more difficult to distinguish between mass-step and survey-selection effects as they become entangled. On the other hand, bias corrections are applied separately after the mass-step correction in JLA, so the mass step is more directly visible in the data.

In this work, the historical development of SNe Ia standardization is traced, from stretch and color corrections to the implementation of the mass-step and bias corrections. Results from three major surveys, JLA, Pantheon+, and DES-SN5YR, are compared to assess the consistency of the mass-step correction and its implications for cosmological parameters, paying particular attention to the role of bias corrections and selection effects.

While previous works investigated the host-galaxy mass-step within individual SN Ia surveys, this study directly compares how the mass-step is implemented, coupled to bias corrections, and computed across three representative surveys: JLA, Pantheon+ and DES-SN5YR. By reconstructing “mass-step removed” Hubble residuals and accounting for the reported mass-step uncertainties, this work aims to provide a comparative investigation on how survey-dependent bias-correction methods impact the visualization and recoverability of the mass-step.

METHODS AND MATERIALS

In this section, an overview of the theoretical framework of translating the observed SN Ia light-curves into cosmological parameters is first provided.

Next, the details on the three publicly available datasets analyzed in this work are presented. Finally, the mass-step reconstruction pipeline, accounting for uncertainties in both the published mass-step values as well as in the distance moduli, is illustrated.

Theoretical Framework

As mentioned in the Introduction, the standardized SN Ia brightnesses can be used to obtain cosmological parameters. In DES-SN5YR, for example, each set of multi-band light-curves was used to obtain the empirical distance modulus with the Tripp equation (10), given as:

$$\mu_{obs,i} = m_{x,i} - M + \alpha x_{1,i} - \beta c_i + \gamma G_{host,i} - \Delta\mu_{bias,i},$$

for the i th SN Ia using the SALT3 light-curve fitter (11, 12, 13) that provides the following fitted parameters: flux amplitude (x_0) with $m_x = -2.5 \log_{10}(x_0)$, stretch (x_1), and color (c). Here, α and β are globally determined parameters, meaning they are kept constant for each SN Ia within a survey. The absolute magnitude M , degenerate with the Hubble constant, is treated as a nuisance parameter and marginalized over.

The empirical distance modulus includes corrections for stretch and color, as well as a host-galaxy stellar mass-dependent γG_{host} . G_{host} is taken to be $+1/2$ if the host is above the mass-step, and $-1/2$ if below the mass step. Selection biases are corrected for with $\Delta\mu_{bias}$ derived from the BEAMS with Bias Corrections (BBC) method (14).

Some selection effects that the BBC framework, a simulation-based method to correct for selection effects, accounts for include the Malmquist bias, in which flux-limited surveys detect intrinsically brighter objects at high redshift, and host-galaxy bias, which are selection effects in which supernova detection and follow-up efficiency depend on host properties, leading to a redshift-dependent sampling of host environments that biases distances due to the mass-luminosity correlation.

The theoretical distance modulus is given by $\mu = m$

$$- M = 5 \log \left(\frac{d_L}{10 \text{ pc}} \right),$$

with m being the apparent magnitude

and M being the absolute magnitude. To note, for a spatially flat universe ($\Omega_k = 0$, $\Omega_m + \Omega_\Lambda = 1$), where Ω_k describes the curvature of the universe, Ω_m represents the fraction of matter (both dark and ordinary), and Ω_Λ represents the fraction of dark energy (assumed to be a cosmological constant), the luminosity distance is given

$$\text{as: } d_L(z) = \frac{c(1+z)}{H_0} \int_0^z \frac{dz'}{E(z')}. \text{ Here, } c \text{ is the speed of light,}$$

z is the redshift, H_0 is the Hubble constant, representing the current expansion rate of the universe e , and $E(z')$, the dimensionless Hubble parameter, is defined in flat Λ CDM as $\sqrt{\Omega_{m,0}(1+z')^3 + \Omega_{\Lambda,0}}$, where $\Omega_{\Lambda,0} + \Omega_{m,0} = 1$. This equation demonstrates how the luminosity distance is related to cosmological parameters of the universe.

$\Omega_{m,0}$ and $\Omega_{\Lambda,0}$ represent the matter density and dark energy density at present. A higher $\Omega_{m,0}$ decreases d_L for a given z , as gravity slows expansion. $\Omega_{\Lambda,0}$ represents dark energy or vacuum energy. Given the assumption of flatness, where $\Omega_{\Lambda,0} + \Omega_{m,0} = 1$, a lower $\Omega_{m,0}$ value results in a higher $\Omega_{\Lambda,0}$, leading to a greater acceleration of the expansion of the universe and a higher d_L . H_0 , the Hubble constant, sets the overall scale of the luminosity distance, and appears in the equation for d_L as an overall scaling factor. In Figure 2, an SN Ia Hubble diagram is shown, or a plot of the distance moduli of the different SNe Ia against the redshift values.

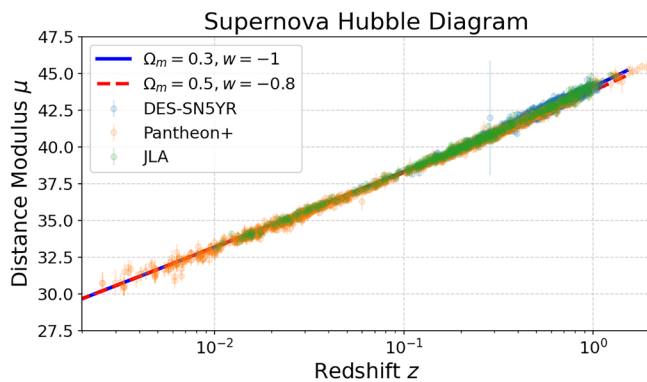


Figure 2. Hubble Diagram for the datasets used in this work from the DES-SN5YR, Pantheon+, and JLA official data release. Uncertainties are statistical only. Lines denote theory curves computed with different model assumptions. The blue line represents a theoretical model with the matter density $\Omega_m = 0.3$, and the dark energy equation of state $w = -1$, while the red dashed line represents $\Omega_m = 0.5$ and $w = -0.8$. All three surveys are roughly in agreement with $\Omega_m = 0.3$ and $w = -1$.

In Figure 3, the Hubble residuals, defined as $\mu_{observed} - \mu_{model}$, are shown for three representative surveys - DES-SN5YR, Pantheon+ and JLA using publicly available data. The Hubble diagram and Hubble residuals will be used to illustrate the dependency of SN Ia brightnesses on host-galaxy stellar mass. The initial standardization of the cosmology samples of JLA, Pantheon+, and DES-SN5YR is performed using the aforementioned Tripp equation. As shown in Figure 2, while all three datasets

align closely with a flat Λ CDM cosmology with $\Omega_m = 0.3$, the Hubble residuals in Figure 3 reveal underlying systematic trends.

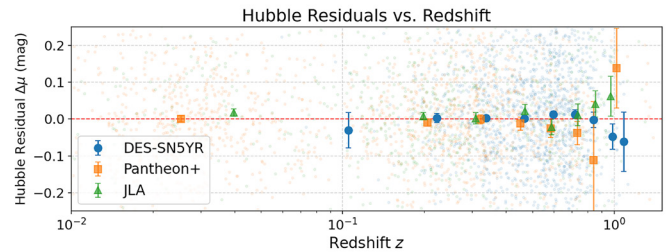


Figure 3. Hubble residuals vs. redshift for the three different surveys used in this work. Hubble residuals are defined as $\Delta\mu = \mu_{observed} - \mu_{model}$, where μ_{model} is calculated using the best-fit model parameters for each survey. While there is some scatter, the binned Hubble Residuals are consistent with zero when averaged across the redshift range and uncertainties are considered for all three surveys. Error bars denote the uncertainty on the median Hubble residual in each redshift bin, and account for the scatter within each bin, as well as the propagated statistical uncertainties of the individual SN Ia distance moduli.

Analyzed Datasets

The three main datasets covered in this paper are the JLA (8), Pantheon+ (9, 15), and DES-SN5YR (5, 16) surveys. The JLA survey combines several datasets, including the Supernova Legacy Survey (SNLS), the Sloan Digital Sky Survey Supernova Survey (SDSS), low-redshift supernova samples, and Hubble Space Telescope Supernova Observations (HST). The JLA sample comprises an extended sample of 740 SNe Ia, with a redshift range of . The observational quantities used in this paper include the redshift, peak apparent magnitude, stretch parameter, color parameter, and host galaxy stellar mass. The SALT2 model (11) is used to fit the light-curves to obtain the stretch and color parameters with the host galaxy mass-step, and bias corrections are applied subsequently.

The Pantheon+ survey covers datasets built on the Pantheon survey, including updated spectroscopically confirmed SNe Ia. Pantheon+ combines datasets from 18 different samples, including: the Foundation Supernova Survey, the Swift Optical/Ultraviolet Supernova Archive (SOUSA), the first sample from the Lick Observatory Supernova Search (LOSS1), the second sample from LOSS (LOSS2), and the Dark Energy Survey (DES)

3 Year Analysis. The redshift range for the entire Pantheon+ survey is $0.001 < z < 2.26$, and it uses ~1700 SNe in their Hubble diagram. The measurements in this paper include the redshifts, standardized magnitudes, light-curve parameters, and the covariance matrices. The BEAMS with Bias Corrections framework is used to correct for selection biases.

The Dark Energy Survey Supernova Program collected DES-SN5YR, observed using the Victor M. Blanco Telescope and the Dark Energy Camera. DES-SN5YR consists of the primary dataset from the full 5 years of DES SNe, along with historical SNe datasets such as CfA3, CfA4, the Carnegie Supernova Project, and the Foundation SN sample. For its observational strategy, it used repetitive imaging of selected deep fields in the g, r, i, z (shorter to longer wavelength-filters) photometric bands. It uses 1800 SNe, and DES-SN5YR consists mostly of photometric samples, meaning they are not necessarily spectroscopically confirmed SNe Ia but are classified based on $griz$ photometry. Multi-band photometry, host-galaxy redshifts, and light-curve parameters are measured, with light curves modeled using SALT3. For bias corrections, DES-SN5YR uses simulation-based bias corrections and the BBC likelihood method similar to Pantheon+. This two-stage statistical technique uses simulations to correct for selection bias and to create a Hubble diagram while excluding potential contaminants in the data. Table 1 summarizes key characteristics for each of the surveys used in this analysis.

Reconstructing the Mass-Step

Publicly available data from JLA (17), Pantheon+ (18), and DES-SN5YR (19) are used to construct the Hubble diagram and Hubble residuals to illustrate the dependency of SN Ia brightnesses on host-galaxy stellar mass. All analyses are performed using Python in a Jupyter Notebook environment. The pandas and astropy.io.fits packages are used to read and organize the SN Ia and host-galaxy information, while numpy is used for numerical calculations including luminosity distances, Hubble residuals, Monte Carlo uncertainty propagation, and statistical binning. Figures are created using matplotlib.pyplot.

The publicly released DES-SN5YR and Pantheon+ distance moduli already include light-curve, host mass-step, and bias corrections. JLA, on the other hand, provides light-curve parameters and correction terms separately, which allows the distance moduli to be reconstructed directly from the SALT2 parameters and covariance matrices. For JLA, the distance modulus uncertainties are computed by propagating uncertainties and covariance terms associated with the apparent magnitude, stretch, and the color parameters while for DES-SN5YR and Pantheon+, the given ‘MU_ERR’ columns (statistical uncertainties only) are used.

In order to explicitly visualize the dependency of the Hubble Residuals on host-galaxy stellar mass, the “mass-step removed” versions of the distance moduli are computed. For DES-SN5YR and Pantheon+, the host mass-step correction term was given as: $\Delta_M = \pm \gamma/2$, with

Table 1. Key characteristics for the Pantheon+, DES-SN5YR, and JLA samples used in this work. Mass-step values are adopted from published results.

Characteristic	Pantheon+	DES-SN5YR	JLA
Approx. Sample Size	About 1700	About 1800	740
Sample Type	Combined spectroscopic compilation	Deep photometric survey	Combined spectroscopic compilation
Redshift Range	$0.001 < z < 2.3$	$0.025 < z < 1.2$	$0.01 < z < 1.3$
Light-Curve Fitter	SALT2/SALT3	SALT3	SALT2
Treatment of Bias Corrections	BBC framework with simultaneous modeling of selection effects and mass-step	BBC framework with simultaneous modeling of selection effects and mass-step	Post-fit simulation-based corrections
Adopted Mass-Step Value	$\gamma = -0.003 \pm 0.007$	$\gamma = 0.038 \pm 0.007$	$\Delta_M = -0.061 \pm 0.012$
Notes	Mass-step largely absorbed into dust/bias-correction framework	Deep photometric survey with strong redshift-dependent bias corrections	Mass-step more directly visible due to simpler correction framework

$\Delta_M > 0$ if the host-galaxy stellar mass is above $10^{10} M_\odot$ and $\Delta_M < 0$ if the host stellar mass is below $10^{10} M_\odot$. $\gamma_{DES} = 0.038 \pm 0.007$ mag and $\gamma_{Pantheon+} = -0.003 \pm 0.007$ mag. For JLA, the mass-step correction term was simply: $\Delta_M = -0.061 \pm 0.012$ mag. The “mass-step removed” distance modulus is then computed as: $\mu_{no-mass} = \mu_{obs} - \Delta_M$, which is exact for JLA since the mass-step and bias corrections are applied separately, but only approximate for DES-SN5YR and Pantheon+, both of which use the BBC framework to simultaneously determine the mass-step and bias corrections.

To account for uncertainties in the adopted mass-step values, Monte Carlo realizations of the host mass-step correction are generated by drawing Δ_M values from Gaussian distributions with means at the published best-fit values and standard deviations corresponding to the reported 1σ uncertainties. These realizations are propagated through the computed “mass-step removed” distance moduli and Hubble residuals.

Hubble residuals are computed with respect to the best-fit Flat-CDM cosmology obtained by each survey. Some figures use redshift- or host-mass-binned medians to reduce scatter and improve visibility of underlying trends, where the uncertainties on binned medians are estimated from the scatter of the SNe Ia within each bin combined with the propagated individual distance modulus uncertainties. The significance of the recovered host-galaxy mass step is estimated using the inverse-variance-weighted mean Hubble residuals above and below the host-galaxy stellar mass step location, $10^{10} M_\odot$. In this analysis, the mass step location is fixed at $10^{10} M_\odot$ as in the original analyses.

RESULTS

In this section, the correlation between host-galaxy stellar mass and the distance modulus μ is explicitly explored. First, the host-galaxy stellar mass is plotted against the redshift for the three surveys considered in this work in Figure 4. The DES-SN5YR sample shows a clear shift towards higher-mass hosts at higher redshifts compared to JLA and Pantheon+, highlighting the different selection functions between surveys utilizing photometric classification (DES-SN5YR) and spectroscopic classification (JLA and Pantheon+). In Figure 5, the mass-step removed binned median Hubble residuals are plotted against the redshift for JLA and DES-SN5YR. The binned Hubble residuals suggest that SNe Ia in hosts more massive than the mass-step location of $10^{10} M_\odot$ are brighter than SNe Ia in hosts

less massive than $10^{10} M_\odot$ for both surveys, after light-curve corrections. Figure 6 shows the mass-step removed binned median Hubble residuals against the host-galaxy stellar mass. While Pantheon+ Hubble residuals show little dependence with the host-galaxy stellar mass as their mass-step correction is absorbed into the bias corrections framework, the Hubble residuals decrease above the mass-step location.

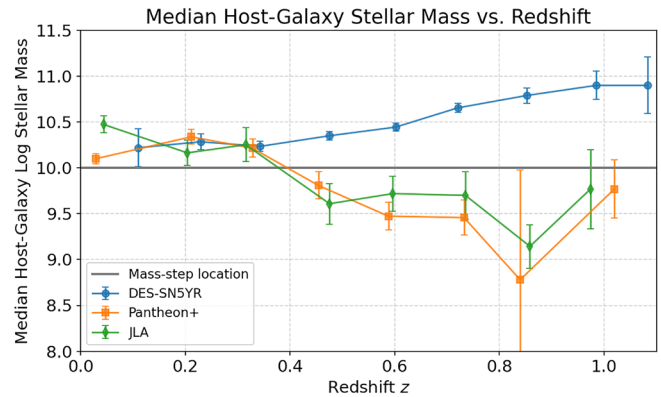


Figure 4. Median host-galaxy log stellar mass vs. redshift across the three different surveys. Pantheon+ and JLA show similar trends. DES-SN5YR exhibits a different behavior likely due to its deeper untargeted photometric strategy for collecting data from SNe Ia. Error bars denote the uncertainty on the median host-galaxy stellar mass in each redshift bin, estimated from the scatter of host-galaxy masses within the bin. $10^{10} M_\odot$ is the mass-step location.

Figures 5 and 6 confirm that SNe in high-mass hosts appear brighter than those in low-mass hosts after stretch and color standardization. As outlined in the Methods and Materials section, the mass-step removed Hubble residuals are reconstructed using Monte Carlo realizations drawn from Gaussian distributions with the means and standard deviations corresponding to the reported value and 1σ uncertainties. The estimated mass-step values for the three surveys using the inverse-variance-weighted mean Hubble residuals are as follows: $\Delta_{M,DES} = 0.037 \pm 0.009$ mag or a 4.1σ significance for DES-SN5YR, $\Delta_{M,Pantheon+} = -0.006 \pm 0.010$ mag or a 0.6σ significance for Pantheon+, and $\Delta_{M,JLA} = -0.059 \pm 0.011$ mag or a 5.3σ significance for JLA, where the sign convention is consistent with each of the surveys (note that the sign for JLA is opposite of DES-SN5YR and Pantheon+). The recovered mass-step values and significance are consistent with the officially reported

values from the three surveys shown in Table 1. The recovered mass-step uncertainties being slightly larger for DES-SN5YR and Pantheon+ compared to the values shown in Table 1 (about 30 to 40%) is likely due to the approximate treatment done for DES-SN5YR and Pantheon+ where the mass-step and bias corrections are assumed to be independent.

One important aspect of the mass-step implementation is its degeneracy with survey selection effects. As shown in Figure 7, the bias correction term $\Delta\mu_{bias}$ becomes dominant at higher redshifts, especially for DES-SN5YR. The results shown in this work indicate that selection effects can influence the mass-step if not properly corrected for. In surveys with limited magnitude, the Malmquist bias tends to prevent fainter SNe Ia at higher redshifts from being detected, distorting the observed SN population. Because the host-galaxy mass-step

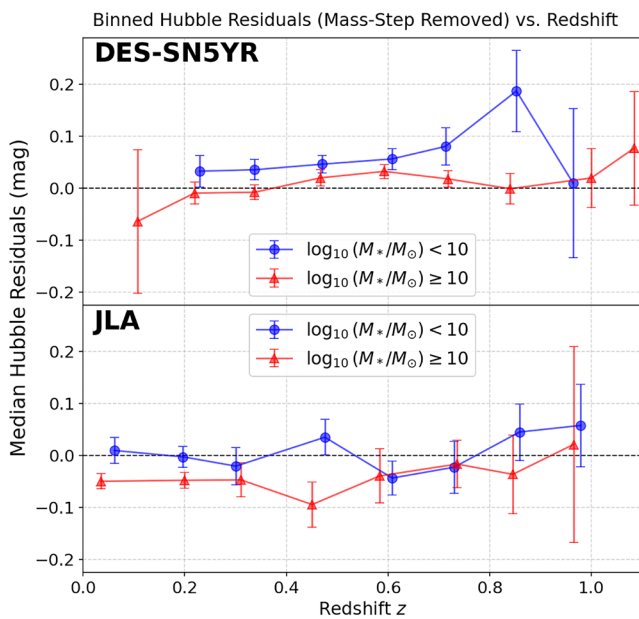


Figure 5. Binned median Hubble residuals (with the mass-step corrections removed) vs. redshift by host-galaxy mass for DES-SN5YR (top) and JLA (bottom). Pantheon+ is not shown as the mass-step is absorbed into bias corrections and therefore more difficult to isolate visually. Hubble residuals are given by $\mu_{observed} - \mu_{model}$, where μ_{model} is calculated using the best-fit model parameters. As in Figure 3, error bars denote the uncertainty on the median Hubble residual in each redshift bin, and account for the scatter within each bin, as well as the propagated statistical uncertainties of the individual SN Ia distance moduli.

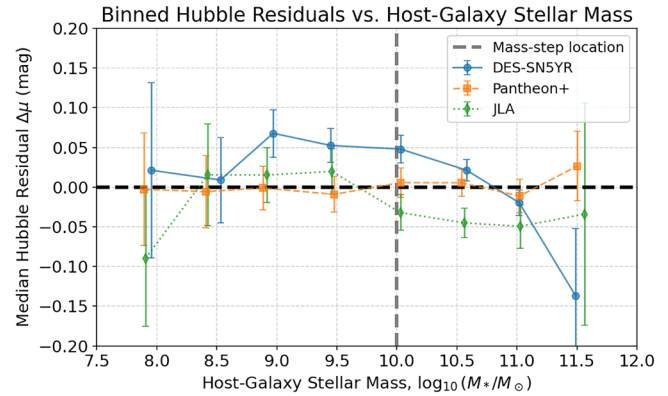


Figure 6. Median mass-step removed binned Hubble residuals vs. host-galaxy log stellar mass across the three different surveys. Pantheon+ shows a consistent Hubble residual throughout all masses as their mass-step is absorbed into bias corrections, while DES-SN5YR and JLA show the Hubble Residuals decreasing at host-galaxy log stellar-mass above 10. Note that at log stellar-mass less than 8, the number of SNe Ia is small. Similar to Figures 3 and 5, error bars denote the uncertainty on the median Hubble residual in each host mass bin, and account for the scatter within each bin, as well as the propagated statistical uncertainties of the individual SN Ia distance moduli.

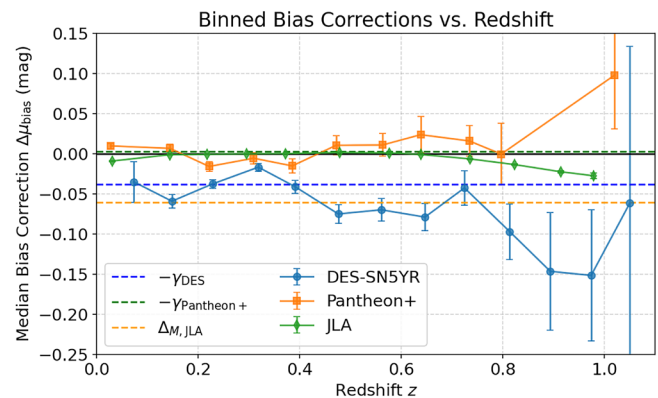


Figure 7. Binned median bias corrections vs. redshift across the three different surveys. The sizes of the mass-step for each survey are shown for reference. JLA is seen to have almost no bias corrections, while DES-SN5YR and Pantheon+ have larger bias corrections especially for supernovae at higher redshifts. This means that for JLA, the mass-step correction is larger than bias corrections while the opposite is true for Pantheon+ and DES-SN5YR. Error bars denote the uncertainty on the median bias correction in each redshift bin, estimated from the scatter within each bin.

indirectly correlates with light-curve properties such as stretch and color, this selection bias might indirectly affect the inferred brightness offset between low- (below $10^{10} M_{\odot}$) and high-mass (above $10^{10} M_{\odot}$) galaxies. In Figure 7, where the bias correction $\Delta\mu_{bias}$ is compared to the size of the mass-step, the bias corrections become comparable or even larger than the mass-step correction at higher redshifts, with the bias correction size reaching ~ 0.08 mag at redshift $z \approx 1$ for DES-SN5YR, which is over twice the size of γ_{DES} . This demonstrates that accurate bias corrections are necessary to avoid altering the determined value of γ from the data. Note that the magnitude of the bias correction term tends to increase at higher redshifts, especially for photometric surveys like DES-SN5YR since the fraction of SNe Ia observed out of the total number of SNe Ia decreases significantly at the higher redshifts. In contrast, the host-galaxy mass-step is typically taken to be the same throughout all redshifts under the assumption that SNe Ia at low and high redshifts are affected similarly by its environment. More specifically, for each survey,

Pantheon+

Across $0 < z < 1.0$, the bias corrections increase gradually with redshift but seemingly remain uncorrelated with the host mass as the Pantheon+ analysis absorbs the mass-step into their dust model. As a result, environmental standardization and bias corrections are thoroughly intertwined, and it is unclear how the dust model and bias corrections affect each other.

DES-SN5YR

In the DES-SN5YR sample, the size of the bias correction term grows significantly with increasing redshift, reaching a value of ~ 0.08 mag at $z \approx 1.0$. At this redshift, the bias correction is twice as large as the host-galaxy mass-step correction term (γ_{DES}). This highlights the importance of accurate bias corrections, as selection effects of comparable magnitude could alter the inferred mass-step parameter if not properly accounted for.

JLA

The JLA survey uses bias corrections derived from simulations, but with a less comprehensive modeling framework than more recent compilations such as Pantheon+ or DES-SN5YR. As a result, the correction structure remains largely dominated by the constant host-mass step, and residual scatter at higher redshifts is somewhat larger than in newer analyses of DES-SN5YR and Pantheon+. This may partially contribute to the

larger apparent mass-step observed in JLA relative to DES-SN5YR.

DISCUSSION

By reapplying and reconstructing host galaxy mass-steps to the publicly released DES-SN5YR, Pantheon+, and JLA datasets, values that are broadly consistent with those originally reported for these samples are recovered. This agreement suggests that the mass-step values are coherent at the population level, even when approximated outside the full bias-correction pipelines. However, this analysis also demonstrates that the mass-step effect cannot be clearly separated from the bias-correction procedures used in modern supernova analyses.

For instance, Pantheon+ uses a BBC framework, in which bias corrections are derived from end-to-end simulations and applied to the standardized distance moduli, while the host-galaxy mass step is constrained simultaneously within a global likelihood that includes these corrections. This results in a more coupled treatment of selection effects and population-level dependencies, where the inferred mass-step is not isolated from the bias-correction procedure.

The comparison between Pantheon+ and DES-SN5YR further illustrates this point. Their implementations of the mass-step slightly differ, with Pantheon+ absorbing the mass-step into their dust model, while DES-SN5YR allows for more direct parameter-level interpretation using the standard Tripp equation. The differences in the recovered values for the mass-step suggest that Δ_M captures a real underlying population effect, but its precise value remains pipeline-dependent. This distinction is particularly important in the context of more recent works (19, 20, 21), which emphasize that small systematic differences in supernova standardization can significantly impact joint constraints with CMB and BAO data, especially in models allowing a time-evolving dark energy. The findings in this work suggest that inconsistent or approximate treatments of the mass-step, especially across different datasets from separate surveys, can introduce subtle but non-negligible biases in cosmological inference.

As with any observational cosmology study, the design of the current study is subject to limitations. First, because the mass-step correction in Pantheon+ and DES-SN5YR is coupled to bias-correction procedures, the approach in this analysis of removing and reintroducing the mass-step into the publicly-released distance moduli constitute an approximate post-processing treatment. In

the original Pantheon+ and DES-SN5YR analyses, the host mass-step correction is determined from a global fitting framework that also determines selection effects and survey-dependent bias corrections simultaneously, meaning that the mass-step is not strictly separable from these other quantities. As such, the reconstructed “mass-step removed” Hubble residuals presented in this work do not fully recover pre-corrected SN Ia distance moduli. Second, this work relies exclusively on publicly available data rather than re-running the full light-curve fitting and BBC pipelines. As a result, this work is unable to test alternative implementations of the mass-step or evaluate its dependence on survey-specific modeling choices. Consequently, the mass-step values reconstructed in this work should primarily be interpreted as phenomenological trends rather than fully independent remeasurements. Third, although the uncertainties from the published mass-step values are propagated using Monte Carlo realizations, this work does not include the full covariance from the original cosmological analyses, meaning that systematic uncertainties are underestimated.

Finally, this work does not attempt to model redshift evolution of the mass-step, which has been suggested in more recent analyses. If the mass-step amplitude evolves with redshift or depends on additional host-galaxy properties, the simple treatment presented in this work could obscure a more complicated astrophysical behavior.

CONCLUSION

In this work, the recoverability of the mass-step is investigated by reintroducing it into the publicly-released supernova datasets accounting for the 1σ uncertainties. While the values recovered are consistent with the Pantheon+, JLA, and DES-SN5YR data, this agreement does not imply full equivalence with the original analyses, as the mass-step is entangled with bias-correction procedures. This highlights a key limitation in treating the mass-step as an independent, additive correction. As SN Ia datasets are increasingly combined with other cosmological probes, ensuring consistent and physically meaningful interpretations of host-galaxy effects will be essential for robust inference in the future.

REFERENCES

1. Chandrasekhar S. The maximum mass of ideal white dwarfs. *Astrophysical Journal*. 1931; 74: 81-82. <https://doi.org/10.1086/143324>

2. Riess AG, Filippenko AV, Challis P, Clocchiatti A, *et al.* Observational Evidence from Supernovae for an Accelerating Universe and a Cosmological Constant. *The Astronomical Journal*. 1998; 116 (3): 1009-38. <https://doi.org/10.1086/300499>
3. Perlmutter S, Aldering G, Goldhaber G, Knop RA, *et al.* Measurements of Ω and Λ from 42 High-Redshift Supernovae. *The Astrophysical Journal [Internet]*. 1999 Jun [cited 2026 Mar 14]; 517 (2): 565-86. <https://doi.org/10.1086/307221>
4. Perlmutter S, Aldering G, Valle MD, Deustua S, *et al.* Discovery of a supernova explosion at half the age of the Universe. *Nature*. 1998 Jan 1; 391 (6662): 51-4. <https://doi.org/10.1038/34124>
5. Abbott DC, Acevedo M, Agüena M, Alarcon A, *et al.* The Dark Energy Survey: Cosmology results with ~ 1500 new high-redshift type Ia supernovae using the full 5 yr data set. *The Astrophysical Journal Letters*. 2024 Sep 1; 973 (1): L14.
6. Rykoff ES, Tucker DL, Burke DL, Allam SS, *et al.* The dark energy survey six-year calibration star catalog. arXiv preprint arXiv:2305.01695. 2023 May 2.
7. Sullivan M, Conley A, Howell DA, Neill JD, *et al.* The dependence of Type Ia Supernovae luminosities on their host galaxies. *Monthly Notices of the Royal Astronomical Society*. 2010 Jul 19; 406 (2): 782-802. <https://doi.org/10.1111/j.1365-2966.2010.16731.x>
8. Betoule M, Kessler R, Guy J, Mosher J, *et al.* Improved cosmological constraints from a joint analysis of the SDSS-II and SNLS supernova samples. *Astronomy & Astrophysics*. 2014 Aug 1; 568: A22.
9. Brout D, Scolnic D, Popovic B, Riess AG, *et al.* The Pantheon+ analysis: cosmological constraints. *The Astrophysical Journal*. 2022 Oct 1; 938 (2): 110.
10. Tripp R, Branch D. Determination of the Hubble Constant Using a Two-Parameter Luminosity Correction for Type Ia Supernovae. *The Astrophysical Journal*. 1999 Nov; 525 (1): 209-14. <https://doi.org/10.1086/307883>
11. Guy J, Astier P, Nobili S, Regnault N, Pain R. SALT: a spectral adaptive light curve template for type Ia supernovae. *Astronomy & Astrophysics*. 2005 Dec 1; 443 (3): 781-91. <https://doi.org/10.1051/0004-6361:20053025>
12. Guy J, Astier P, Baumont S, Hardin D, *et al.* SALT2: using distant supernovae to improve the use of type Ia supernovae as distance indicators. *Astronomy & Astrophysics*. 2007 Apr 1; 466 (1): 11-21. <https://doi.org/10.1051/0004-6361:20066930>
13. Kenworthy WD, Jones DO, Dai M, Kessler R, *et al.* SALT3: An improved type Ia supernova model for measuring cosmic distances. *The Astrophysical Journal*. 2023 Jun 1; 950 (1): L14.

- Journal*. 2021 Dec; 923 (2): 265. <https://doi.org/10.3847/1538-4357/ac30d8>
14. Kessler R, Scolnic D. Correcting type Ia supernova distances for selection biases and contamination in photometrically identified samples. *The Astrophysical Journal*. 2017 Feb 10; 836 (1): 56. <https://doi.org/10.3847/1538-4357/836/1/56>
 15. Scolnic D, Brout D, Carr A, Riess AG, *et al*. The Pantheon+ analysis: the full data set and light-curve release. *The Astrophysical Journal*. 2022 Oct 1; 938 (2): 113. <https://doi.org/10.3847/1538-4357/ac8b7a>
 16. Vincenzi M, Brout D, Armstrong P, Popovic B, *et al*. The dark energy survey supernova program: Cosmological analysis and systematic uncertainties. *The Astrophysical Journal*. 2024 Nov 1; 975 (1): 86.
 17. Dark Energy Survey Supernova Program. DES-SN5YR Data Release. Available from: <https://github.com/des-science/DES-SN5YR> (accessed on 2025-12-11)
 18. Pantheon+ SH0ES Team. Pantheon+ Data Release. Available from: <https://github.com/PantheonPlus> SH0ES/DataRelease (accessed on 2025-12-11)
 19. Centre de Données astronomiques de Strasbourg (CDS). Joint Light-curve Analysis (JLA) Data Release. Available from: <https://cdsarc.cds.unistra.fr/viz-bin/cat/J/MNRAS/486/L46> (accessed on 2026-1-12).
 20. Efstathiou G. Evolving dark energy or supernovae systematics?. *Monthly Notices of the Royal Astronomical Society*. 2025 Apr; 538 (2): 875-82. <https://doi.org/10.1093/mnras/staf301>
 21. Vincenzi M, Kessler R, Shah P, Lee J, *et al*. Comparing the DES-SN5YR and Pantheon+ SN cosmology analyses: investigation based on 'evolving dark energy or supernovae systematics'?. *Monthly Notices of the Royal Astronomical Society*. 2025 Aug; 541 (3): 2585-93. <https://doi.org/10.1093/mnras/staf943>
 22. Hoyt TJ, Rubin D, Aldering G, Perlmutter S, Cuceu A, Gupta R. Union3. 1: Self-consistent Measurements of Host Galaxy Properties for 2000 Type Ia Supernovae. arXiv preprint arXiv:2601.19424. 2026 Jan 27.